TÜBİTAK

Turk J Elec Eng & Comp Sci, Vol.19, No.6, 2011, © TÜBİTAK
doi:10.3906/elk-1004-4

A Luenberger-sliding mode observer with rotor time constant parameter estimation in induction motor drives

Mustafa Gürkan AYDENİZ*, İbrahim ŞENOL
Department of Electrical Engineering, Yıldız Technical University,
34349 İstanbul-TURKEY
e-mails: aydeniz@yildiz.edu.tr, senol@yildiz.edu.tr

Received: 02.04.2010

Abstract

The performance and efficiency of an induction motor drive system can be enhanced by online estimation of critical parameters such as rotor time constant. A novel Luenberger-sliding mode observer with a parameter adaptation algorithm is proposed in this paper to compensate for the parameter variation effects. The observer is comparably simple and robust relative to the previously developed observers, and yet suitable for online implementation. Simulation studies for the proposed method were conducted in a MATLAB environment. Observer constants and the control parameters were tuned during the simulation studies and used during the experimental study stage. Experimental verification of the developed algorithm was performed with an induction motor using the rotor flux-oriented vector control. The comparative results and related overall conclusions are presented accordingly.

Key Words: *Induction motor, sensorless speed control, motor drive, parameter estimation, observer*

1. Introduction

Induction motors (IMs) are the most preferred electric motors due to having rigid structure, ease of maintenance, and low cost. Although they were hardly used in digital applications until the 1980s because of slow response time and complicated control systems, recently they are used in applications of servo systems since the vector control algorithm has enabled them to have improved response time. The costs can be reduced further compared to other electric drive systems with the sensorless control of IMs (without velocity feedback). Despite the advantage of reduced costs, the complicated structure of IMs, involving parameter variation, causes problems in transient response. This has limited the use of sensorless control for IMs in industrial applications. There have been various efforts from the industry and academia on the structure of observers estimating the motor velocity with the aim of eliminating this limitation. Indirect flux-oriented control was applied to the IM by Hasse in 1968 [1]. In this study, sliding mode control calculations of the motor were obtained by stator currents. On the other hand, direct flux-oriented control was applied by Blaschke in 1971 [2]. While this method was

*Corresponding author: Department of Electrical Engineering, Yıldız Technical University, 34349 İstanbul-TURKEY

applied, Hall effect transducers, sensing windings, and the third harmonic of the stator voltages were used to obtain flux orientation. Joetten and Maeder, using adverse EMF vector, had important improvements on the sensorless vector control in 1983 [3]. Sangwongwanic et al. used the sliding mode control method for direct flux-oriented control in 1990 [4]. Brdys and Du obtained the Luenberger observer in 1991 [5]. Vas et al. used the fuzzy control method with the Luenberger observer in sensorless control in 1995 [6]. Abrate et al. also had a new approach to the Luenberger observer, using the fuzzy method for the coefficients of the gain matrix of the observer in 1999 [7]. Lee et al. also used the Luenberger observer to estimate inertia torque in 2004 [8]. To derive benefit from these successful studies, in this study, a new robust observer was designed with the combination of the sliding mode approach and the Luenberger observer to reduce the adverse affect of the variation of the rotor time constant, which is the most effective parameter. The observer was then used in the rotor flux-oriented vector control of the IM. The mathematical model of the IM, the sliding mode approach, the Luenberger observer structure, and the new observer are demonstrated in Section 2. Simulation setup and parameters, experimental setup and a block diagram of the whole system, control and estimation of the system, and the results are discussed in Section 3. Findings of the simulation and experimental results and future research are presented in the conclusion.

2. Theoretical approach

The mathematical model that represents the steady state and the transient state machine behavior is defined by using space vectors for convenience in calculating. To ease analysis, it is accepted that the motor air gap is smooth, iron permeability is infinite, flux density is perpendicular to the surface, and there is no winding slot effect, iron loss, or point effect. The stator and rotor model of the IM are obtained as below:

$$\frac{d}{dt}\begin{bmatrix} i_{sD} \\ i_{sQ} \end{bmatrix} = -C_1 \begin{bmatrix} i_{sD} \\ i_{sQ} \end{bmatrix} + C_2 \begin{bmatrix} x_r & w_r \\ -w_r & x_r \end{bmatrix} \begin{bmatrix} \Psi_{rd} \\ \Psi_{rq} \end{bmatrix} + C_3 \begin{bmatrix} u_{sD} \\ u_{sQ} \end{bmatrix}, \tag{1}$$

$$\frac{d}{dt}\begin{bmatrix} \Psi_{rd} \\ \Psi_{rq} \end{bmatrix} = \begin{bmatrix} -x_r & -w_r \\ w_r & -x_r \end{bmatrix} \begin{bmatrix} \Psi_{rd} \\ \Psi_{rq} \end{bmatrix} + L_m x_r \begin{bmatrix} i_{sD} \\ i_{sQ} \end{bmatrix}, \tag{2}$$

where:

$$C_1 = \left[\frac{1}{T'_s} + \frac{(1-\sigma)}{T'_r}\right], \quad C_2 = \left[\frac{L_m}{L'_s L_r}\right], \quad C_3 = \frac{1}{L'_s}, \text{ and } x_r = 1/T_r.$$

L_m, L_r, and L_s are the magnetizing, rotor, and stator inductances, respectively. $\mathrm{L}'_s = \mathrm{L}_s - \mathrm{L}^2_m/\mathrm{L}_r$ is the stator transient inductance. The stator and rotor transient time constants are defined as $\mathrm{T}'_s = \mathrm{L}'_s/\mathrm{R}_s$ and $\mathrm{T}'_r = \mathrm{L}'_r/\mathrm{R}_r$, respectively. R_s and R_r are stator and rotor resistances. L'_r is defined as $\mathrm{L}'_r = \mathrm{L}'_r - \mathrm{L}^2_m/\mathrm{L}_s$. The leakage factor, σ, is given as $\sigma = 1 - \mathrm{L}^2_m/(\mathrm{L}_s\mathrm{L}_r)$.

Sensorless vector control was realized by taking the flux and torque as references for the system. θ is angle of the rotor flux vector between the D-axis. This angle value was obtained by the components of the rotor flux vector via the observer. θ is necessary for the transformation between the (D-Q) stationary reference frame and the (d-q) rotating reference frame. The accuracy of the angle is so important that it affects the vector control. A phasor diagram in connection with these transformations is shown in Figure 1.

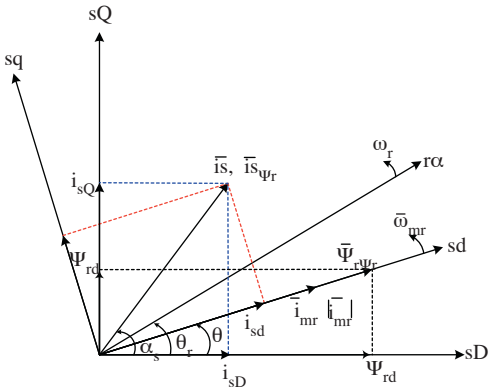

Figure 1. Stator currents in D-Q and d-q axis.

2.1. Observer method

The motor's model can be represented in state space, $\dot{X}(t) = A.X(t) + B.U(t)$, where the state variables A, B, and u are described as follows.

$$X = \begin{bmatrix} i_{sD} & i_{sQ} & \psi_{rd} & \psi_{rq} \end{bmatrix}^T, U = \begin{bmatrix} u_{sD} \\ u_{sQ} \end{bmatrix}, B = \begin{bmatrix} \frac{1}{L_s'} & 0 & 0 & 0 \\ 0 & \frac{1}{L_s'} & 0 & 0 \end{bmatrix}^T \tag{3}$$

$$A = \begin{bmatrix} -[1/T'_s + (1-\sigma)/T'_r]\, I_2 & [L_m/(L'_s L_r T_r)]\, [I_2/T_r - w_r J] \\ (L_m/T_r) I_2 & -(1/T_r) I_2 + w_r J \end{bmatrix} \tag{4}$$

I_2 is a 2 $\times$ 2 identity matrix and the J matrix is:

$$J = \begin{bmatrix} 0 & -1 \\ 1 & 0 \end{bmatrix}. \tag{5}$$

To estimate the rotor speed, the Luenberger observer method can be used and given as:

$$\frac{d\hat{x}}{dt} = \hat{A}x + Bu + G(i_s - \hat{i}_s). \tag{6}$$

These dynamics are similar to the motor model, except $\hat{x}$, $\hat{A}$, G, and $\hat{i}_s$. The convergence properties have been well studied in the literature [6-8]. $\hat{A}$ can be partitioned as:

$$\widehat{A} = \begin{bmatrix} -[1/T'_s + (1-\sigma)/T'_r]\, I_2 & [L_m/(L'_s L_r T_r)] \left[I_2/T_r - \widehat{w}_r J\right] \\ (L_m/T_r) I_2 & -(1/T_r) I_2 + \widehat{w}_r J \end{bmatrix}. \tag{7}$$

The G matrix in the observer equation is known as the observer gain matrix and is written as a 2 $\times$ 4 matrix with constant values [14].

2.2. The new approach

Nonlinear systems like induction motors can be presented as state space models, shown below.

$$\dot{x} = A(x,t) + B(x,t).u(t), \tag{8}$$

where x$\in$R^n, A$\in$F ^{n}, u$\in$R^m, rank(B (x, t)) = m, u $\in$ [u$_{min}$, u$_{max}$].

Selection of the switching function of m items for sliding mode,

$$S = \{x : \phi(t) - \varphi(x) = s(x,t) = 0\} \tag{9}$$

$\phi(t)$, is a function of desired state values, $\phi(t) = f(x^r)$. Because reference values are a function of time, they are denoted as $\phi(t)$. Furthermore, $\varphi(x)$ is a function of state variables.

The sliding surface S$_{(mx1)}$ for the given system is defined by Eq. (8), in which functions are defined as:

$$\phi(t) = H.x^r, \varphi(x) = H.x \tag{10}$$

$$s(x,t) = \phi(t) - \varphi(x) = G.(x^r - x). \tag{11}$$

H$_{(mxn)}$ is a coefficient matrix that establishes the slop of the sliding surface. H is usually defined as a diagonal matrix; entries are taken as positive defined coefficients for making zero state errors ($\varepsilon_i = x_i^r - x_i$) and are obtained from Eq. (12).

$$s_i = \left(\frac{d}{dt} + h_i\right)\varepsilon_i \tag{12}$$

Consequently, ε_i goes to zero when s_i goes to zero. V is a scalar function of S and Lyapunov functions with its derivative chosen as:

$$V(S) = \frac{S^T.S}{2}, \dot{V}(S) = -S^T.D.sign(S). \tag{13}$$

From the Lyapunov stability criteria, V(S) is absolutely positively defined and $\dot{V}(S)$ is absolutely negatively defined. D$_{(mxm)}$ is a positively defined diagonal gain matrix and sign(S) is a signum function.

$$sign(S) = [sign(S_1).....sign(S_m)]^T \tag{14}$$

$$sign(S_i) = \begin{cases} +1 & S_i > 0 \\ 0 & S_i = 0 \\ -1 & S_i < 0 \end{cases} \tag{15}$$

The derivative of Eq. (11), which defines S(x), and the system equation, Eq. (8), are used to obtain Eq. (16).

$$\dot{S} = \dot{\phi}(t) - \frac{\partial S_a}{\partial x}\dot{x} = \dot{\phi}(t) - H.(A(x) + Bu) \tag{16}$$

The control that provides the derivative of the slide function zero is called an equivalent control.

$$u_{eq}(t) = -(H.B)^{-1}\left(G.A(x) - \dot{\phi}(t)\right) \tag{17}$$

The control rule can be written as:

$$u(t) = u_{eq}(t) + (H.B)^{-1}.D.sign\left(S(x,t)\right). \tag{18}$$

A disadvantage of the equivalent control is that it contains numerous operations. To solve this problem, a calculation method was improved, based on estimation of the equivalent solution u$_{eq}$. In this method, a first-order filter is used for estimation. These filter dynamics are:

$$\tau_i \dot{\hat{u}}_{eq_i}(t) + \hat{u}_{eq_i}(t) = \hat{u}_i(t) \quad , \quad \hat{u}_{eq_i} = \frac{1}{\tau_i.s + 1}u_i, \tag{19}$$

where $\hat{u}_{eq_i}$ is the estimated u_{eq_i} and "s" is the Laplace operator. Consequently, the control rule can be written as:

$$u(t) = \hat{u}_{eq}(t) + (H.B)^{-1}.D.h(S). \tag{20}$$

Using a linear function at h(S) and implementing Euler approximation, the derived rule can be used in estimation in discrete time.

$$u_{(t)} = u_{(t-\delta t)} + \frac{(H.B)^{-1}}{\delta t}\left((D.\delta t + 1).S_{(t)} - S_{(t-\delta t)}\right) \tag{21}$$

The rotor time constant vector matrix can be defined as part of Eq. (1), and can be written as:

$$f = \begin{bmatrix} f_D \\ f_Q \end{bmatrix} \hat{=} \begin{bmatrix} x_r & w_r \\ -w_r & x_r \end{bmatrix} \quad \begin{bmatrix} \Psi_{rd} \\ \Psi_{rq} \end{bmatrix}_; \tag{22}$$

thus, the estimated values of the stator model are:

$$\frac{d}{dt}\begin{bmatrix} \hat{i}_{sD} \\ \hat{i}_{sQ} \end{bmatrix} = -C_1 \begin{bmatrix} \hat{i}_{sD} \\ \hat{i}_{sQ} \end{bmatrix} + C_2 \begin{bmatrix} \hat{f}_D \\ \hat{f}_Q \end{bmatrix} + C_3 \begin{bmatrix} u_{sD} \\ u_{sQ} \end{bmatrix}. \tag{23}$$

The difference of these 2 models can be obtained by subtracting Eq. (23) from Eq. (1):

$$\begin{bmatrix} \Delta\dot{i}_{sD} \\ \Delta\dot{i}_{sQ} \end{bmatrix} = -C_1 \begin{bmatrix} \Delta i_{sD} \\ \Delta i_{sQ} \end{bmatrix} + C_2 \begin{bmatrix} \Delta f_D \\ \Delta f_Q \end{bmatrix}. \tag{24}$$

The variation of currents and its derivation can be obtained as zero by controlling the vector $\hat{f}$ ($\Delta i_s = 0, \Delta\dot{i}_s = 0$) [11, 13].This control vector, $\hat{f}$, can be written as:

$$\hat{f} = \begin{bmatrix} \hat{f}_D \\ \hat{f}_Q \end{bmatrix} \hat{=} \begin{bmatrix} \beta & \hat{w}_r \\ -\hat{w}_r & \beta \end{bmatrix} \quad \begin{bmatrix} \hat{\Psi}_{rd} \\ \hat{\Psi}_{rq} \end{bmatrix} = \begin{bmatrix} \hat{\Psi}_{rd} & \hat{\Psi}_{rq} \\ \hat{\Psi}_{rq} & -\hat{\Psi}_{rd} \end{bmatrix} \quad \begin{bmatrix} \beta \\ \hat{w}_r \end{bmatrix}. \tag{25}$$

β in Eq. (25) is the control variable, which tunes the variations of the rotor time constant. Because the variation of the flux components is slower than that of the current, this tune operation can be written like Eq. (21):

$$\beta_{(t)} = \beta_{(t-T)} + \frac{L'_s.L_r}{L_m.T.\left|\hat{\Psi}_r\right|}. \begin{bmatrix} \cos\hat{\theta}.\left[(D.T+1).\Delta i_{sD(t)} - \Delta i_{sD(t-T)}\right] \\ +\sin\hat{\theta}.\left[(D.T+1).\Delta i_{sQ(t)} - \Delta i_{sQ(t-T)}\right] \end{bmatrix}. \tag{26}$$

Δ is the difference in real and estimated values ($\Delta i_{sD} = i_{sD} - \hat{i}_{sD}$ and $\Delta i_{sQ} = i_{sQ} - \hat{i}_{sQ}$).

In this study, the new approach incorporates β ınto the observer matrix. β reduces the adverse effect caused by the variation of the rotor time constant. Rotor resistance can change from nominal values by about 20%-50% [9, 10]. Although the observer dynamics are similar to those given in Eq. (6), the $\hat{A}$ matrix with β can be described as:

$$\widehat{A} = \begin{bmatrix} -\left[1/T'_s + (1-\sigma)/T'_r\right] I_2 & \left[L_m/(L'_s L_r)\right] \left[\beta I_2 - \widehat{w}_r J\right] \\ L_m \beta I_2 & -\beta I_2 + \widehat{w}_r J \end{bmatrix}. \tag{27}$$

To reduce the calculation time of the algorithm, 4 entries of the observer gain matrix are taken as 0. Other entries are constant, as shown below.

$$\begin{aligned} &g_{12} = g_{21} = g_{31} = g_{41} = 0 \\ &g_{11} = g_{22} = c_1 \\ &g_{32} = -g_{42} = c_2 \end{aligned} \tag{28}$$

Speed is calculated with an error signal, which is composed of d and q components and can be written as:

$$e_w = \hat{\Psi}_{rq} e_{sD} - \hat{\Psi}_{rd} e_{sQ}, \tag{29}$$

where $e_{sd} = i_{sD} - \hat{i}_{sD}$ and $e_{sq} = i_{sQ} - \hat{i}_{sQ}$.

Next, to accomplish the estimation of the rotor speed, an e_w signal is used (substituted) in the PI controller:

$$\hat{w}_r = K_p e_w + K_i \int (e_w) dt. \tag{30}$$

Figure 2 demonstrates the speed estimation; basically, measured voltage and currents are used for flux and current estimation, and those estimated values are used to estimate motor speed [14].

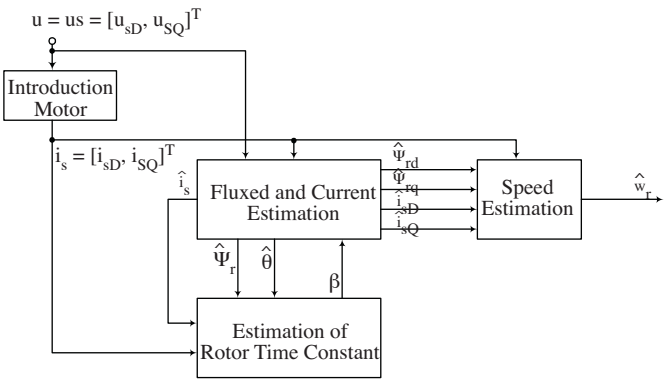

Figure 2. Block diagram of the speed estimation.

3. Experimental studies and results

Since it has been proven in the literature that rotor flux-oriented control has better stability, rotor flux-oriented control, which is basically vector control, was implemented in this study. The shortcoming of this method is that it requires suitable motor structure to measure rotor flux. One way to overcome this is to estimate rotor flux rather than measure it. In this paper, a new observer is proposed to estimate rotor flux and thus the rotor speed. These estimations are used in the vector control. This control block is shown in Figure 3.

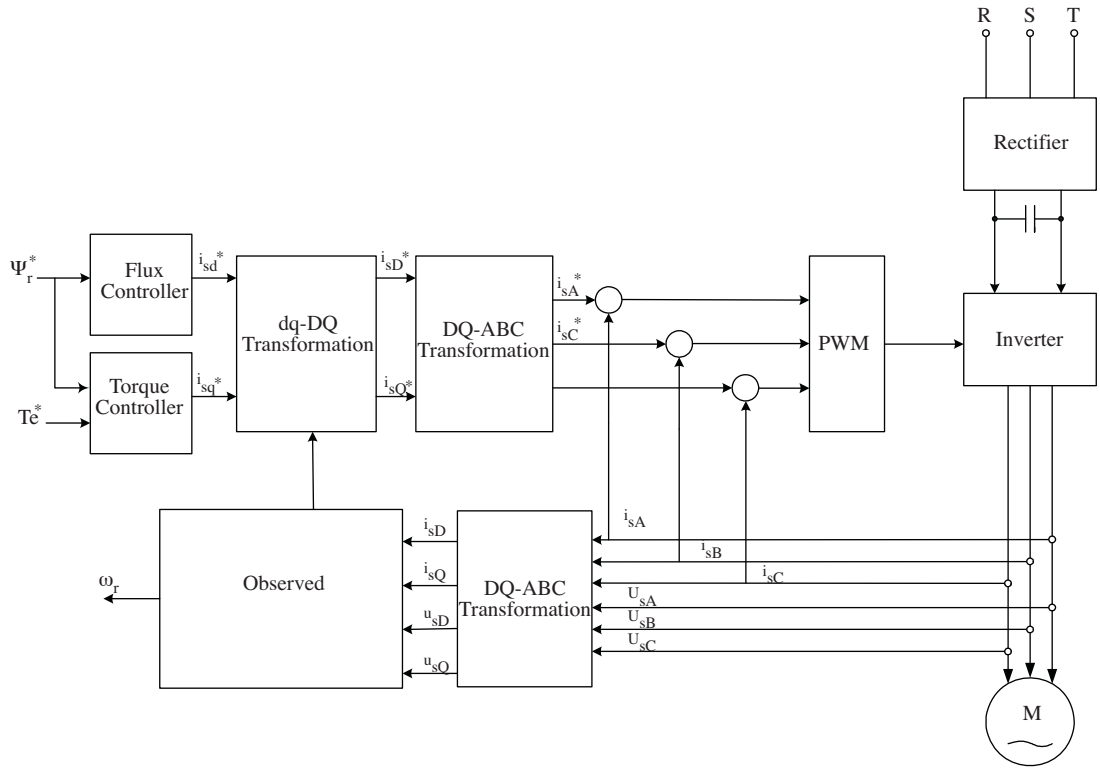

Figure 3. Block diagram of sensorless speed control.

Sensorless vector control is realized by the reference flux and torque as input for the system. θ is the angle of the rotor flux vector between the D-axis. This angle value is obtained by the components of the rotor flux vector via the observer. θ is necessary for the transformation between the stationary reference frame (D-Q) and rotating reference frame (d-q), which is rotating with the rotor flux vector's speed. It is important that the accuracy of the angle value (estimation of the components of the rotor flux vector) affects the vector control. A phasor diagram in connection with these transformations is shown in Figure 1.

In the rotor-flux-oriented control, the rotating axes are determined by the fact that the rotor flux vector is over one of the axes As shown in Figure 1, the rotor flux vector is on the top of the D-axis. Components of the flux vector in the stationary reference frame are shown in the Figure as ψ_{rd} and ψ_{rq} in the D- and Q-axis, respectively. Components of the reference stator current in the stationary reference frame are obtained by a θ angle and flux reference with torque reference used in the rotating reference frame. PWM signals are used switch to IGBTs in inverter to drive the motor; these signals are generated by comparing the measured current with the estimated current [14].

3.1. Simulations

MATLAB was used for calculation and simulation. In the contributed software, the sampling time was 100 μs, and 11,000 loops were used in the software. As a result, the total time of the simulation was 1.1 s. Note that this duration was enough for the steady state status for the motor speed.

Motor parameters were:

$\mathrm{R}_s = 7$, $\mathrm{R}_r = 5.4$, $\mathrm{L}_{ls} = 20 \times 1\mathrm{e}-3$, $\mathrm{L}_{lr} = 20 \times 1\mathrm{e}-3$, $\mathrm{L}_m = 382 \times 1\mathrm{e}-3$, ($\mathrm{L}_s = \mathrm{L}_{ls} + \mathrm{L}_m$, $\mathrm{L}_r = \mathrm{L}_{lr} + \mathrm{L}_m$);

P = 4 (number of the motor poles);

J = 0.01 (inertia of the motor);

V_{dc} = 311 V (DC bus voltage).

Furthermore, the flux reference and torque reference were taken as 0.5 Wb and 2 Nm, respectively.

It should be mentioned that the most effective parameter in the mathematical model of IMs is the rotor time constant. The variation of the rotor time constant has a negative effect for the realization of the sensorless control of the IM. Thus, simulations were carried out for 3 different rotor time constant (T_r) values for the new observer.

The nominal value of the rotor time constant is:

$$T_r = \frac{L_r}{R_r} = \frac{L_{lr} + L_m}{R_r} = \frac{0.402}{5.4} = 0.0744. \tag{31}$$

Simulations were realized for Tr = (Tr)n = 0.0744, Tr = 0.8 × (Tr)n, and Tr = 1.5 × (Tr)n, and it is shown in Figures 4-6 that the estimated speed was obtained from the new observer, the motor speed, and the error between those for Tr = (Tr)n, Tr = 0.8 × (Tr)n, and Tr = 1.5 × (Tr)n, respectively.

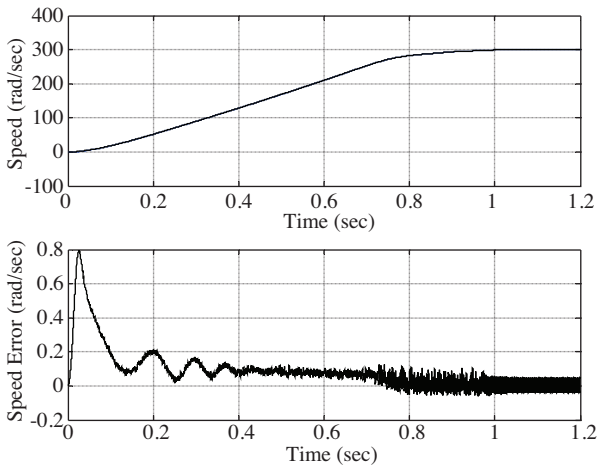

Figure 4. The estimated speed, the motor speed, and the error between the 2 speeds for Tr = (Tr)n = 0.0744.

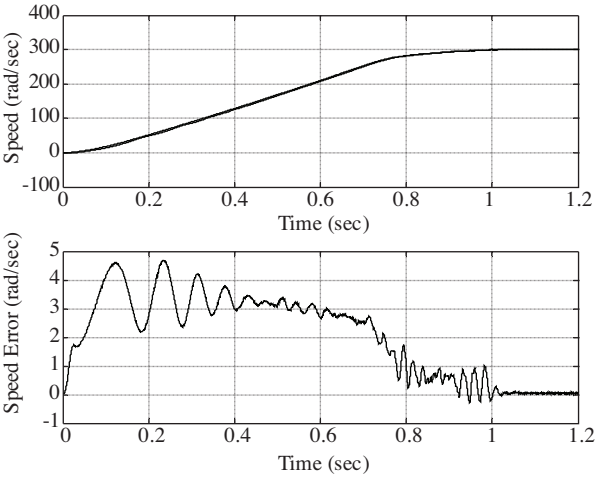

Figure 5. The estimated speed, the motor speed, and the error between the 2 speeds for Tr = 0.8 × (Tr)n.

From the simulations, the motor torque, along with the speed, was also obtained and is shown in Figure 7.

For comparison with conventional observers to prove the effectiveness of the proposed algorithm, similar simulations were carried out with the classical Luenberger observer. Simulations were realized for Tr = 0.8 × (Tr)n and Tr = 1.5 × (Tr)n, and it is shown in Figures 8 and 9 that the estimated speed was obtained from the observer, the motor speed, and the error between those for Tr = 0.8 × (Tr)n and Tr = 1.5 × (Tr)n, respectively.

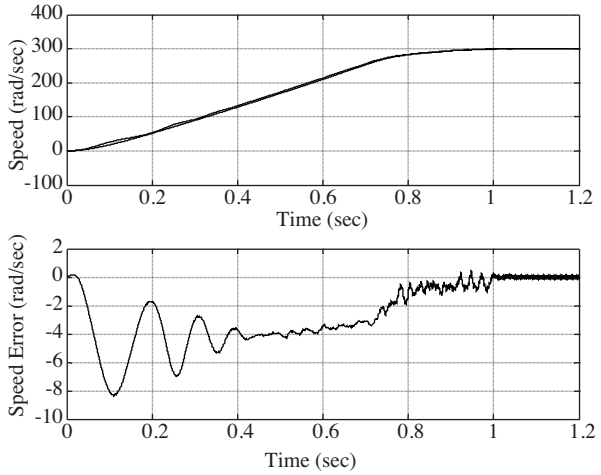

Figure 6. The estimated speed, the motor speed, and the error between the 2 speeds for Tr = 1.5 × (Tr)n.

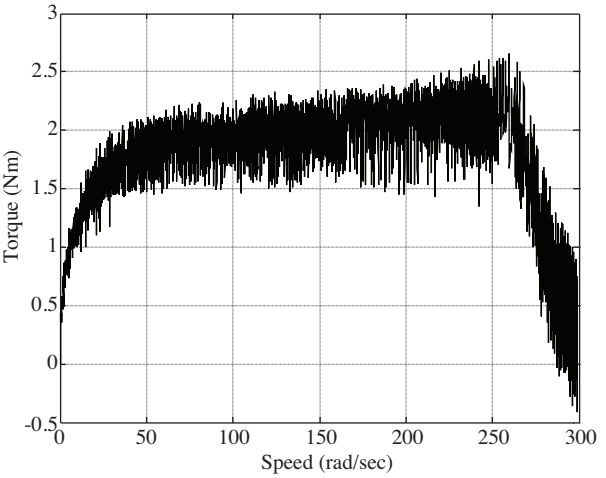

Figure 7. The motor torque along with the speed.

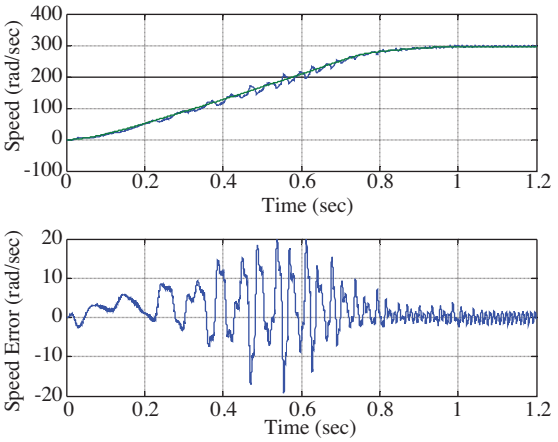

Figure 8. The estimated speed, the motor speed, and the error between the 2 speeds for Tr = 0.8 × (Tr)n in the classical Luenberger observer.

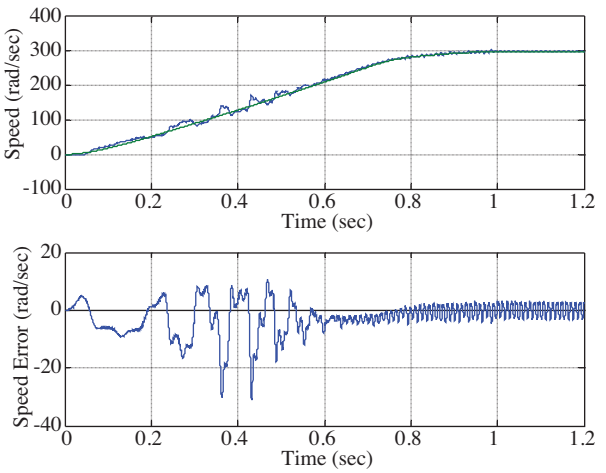

Figure 9. The estimated speed, the motor speed, and the error between the 2 speeds for Tr = 1.5 × (Tr)n in the classical Luenberger observer.

As can be seen from Figure 4 of the proposed algorithm, the estimated speed exactly follows the motor speed when the rotor time constant is kept to the original value, while the speed error is below 1% in the transient condition and around 0.1% at steady state. When the rotor time constant changes, the error grows slightly, by 1%. In the steady state, the error is less than 1% (Figures 5 and 6).

These results are in favor of our proposed algorithm when compared to the classical Luenberger observer, where the error is almost 5% in the transient condition and above 1% in the steady state (Figures 8 and 9).

3.2. Implementation

In the experimental circuit, a 3-phase uncontrolled rectifier (6RI30G160) that produces a DC voltage across the filter capacitor (2200 μF) and an intelligent power module inverter (IPM-7MBP25RA120) were used in the power

circuit. The control algorithm was run with a Pentium-based PC. ADC and the encoder card were connected to the selectable addresses of a standard 64-bit I/O card (DESICION) on the ISA slot of the PC. Control and input/output signals were generated by this card. In the ADC card, a fast analog digital transducer (AD7864) was used. The transducer integrated circuit had 4 channels and sampled the analog inputs simultaneously. The ADC card converted the analog input on a channel to the digital in 1.65 μs.

The speed of the motor was measured by an encoder (RU-4096) at 4096 impulse/cycle with an encoder card. It is clear that in the sensorless control, it is not necessary to use an encoder and an encoder card. In this study, they were used in order to compare the estimated speed with the real speed of the motor. In the encoder card, signal impulses from the encoder were counted and decided the direction of rotation at the same time.

Current and voltages were measured by Hall effect sensors. To measure currents of the motor's 2 current transducers (LTS 15-NP) and the voltage of the DC link, a voltage transducer (LV 25-P) was used. In the realized control system, the control period Ts was chosen as 30 μs. Every 30 μs, 2 phase currents and the DC link voltage were sampled by ADC. To obtain the control period, the PB4 port in the 0x61 address of the PC was used. The control software was written with C code. Calculated switch signals drove the IPM by using the I/O card. The drive circuit was isolated to the PC by using opto-transistors (HCPL 4503). For the drive circuit of the IPM, 4 pieces isolated sources of $\pm$15 V. For the current transducer a source of +5 V was used, and for the voltage transducer, a source of $\pm$15 V. It should be underlined that isolation between the PC and the power circuit was obtained fully.

The desired reference speed value was an input to the control algorithm. The amplitude and the angle of the rotor flux were obtained from the components of the estimated rotor flux. To obtain the angle in this way is very difficult when using a microcontroller, because this process takes much time. Thus, sine and cosine tables were composed in the experiment. Consequently, the tangent of the rotor flux and the transformation of the axis were obtained. After the reference flux and torque, reference stator currents were calculated by using the reference speed value. Comparison of the measured current values and the reference values was used for the drive signals of the IPM by using the hysteresis control method. Band width was taken as 0.1 s in the hysteresis. Estimated values of the rotor time constant (β) were updated in every period of the control. In the estimation of the speed, the components of the estimated rotor flux and the difference between the measured and the estimated stator currents in the DQ-axis were input values. Estimation of the speed was obtained by imposing the signal from a PI controller. PI parameters in the controller were tuned. The experimental block diagram is given in Figure 10 [14].

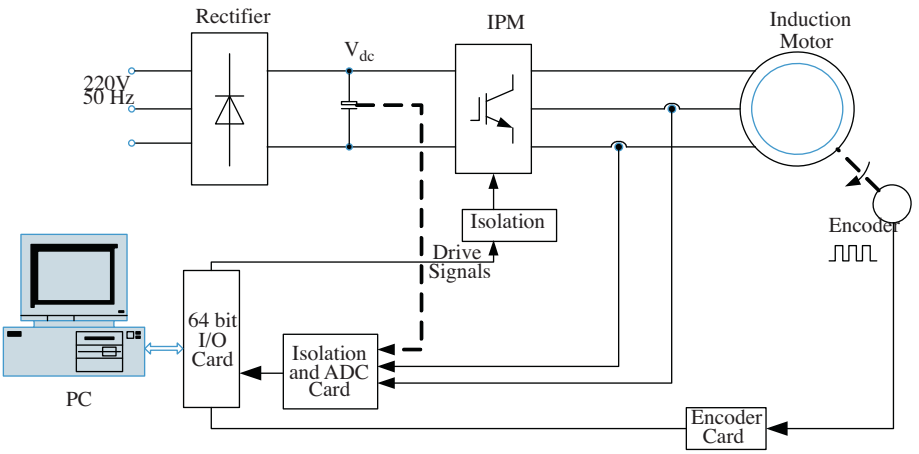

Figure 10. Block diagram of experimental study.

Reference speed values were taken as 250 and 500 rpm. In the control part, 1 cycle was taken as a 5500 period, which means that it was sampled 5500 times. The sampling value was limited because of the capacity of the system. The estimated and the measured values of the speed were taken from the I/O card.

The test rig is presented in Figure 11. Estimated and measured speeds for references of 250 and 500 rpm are shown in Figures 12 and 13.

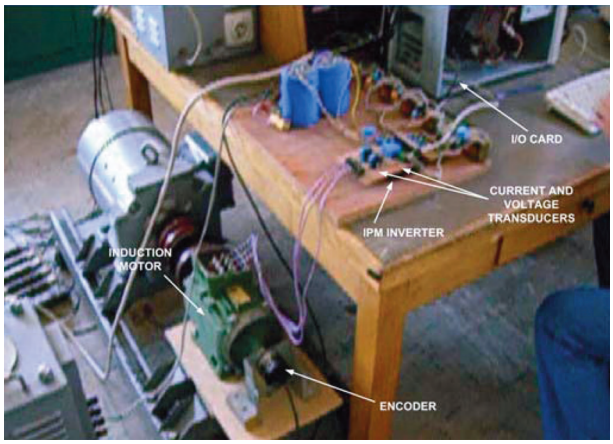

Figure 11. The test rig of the experimental study.

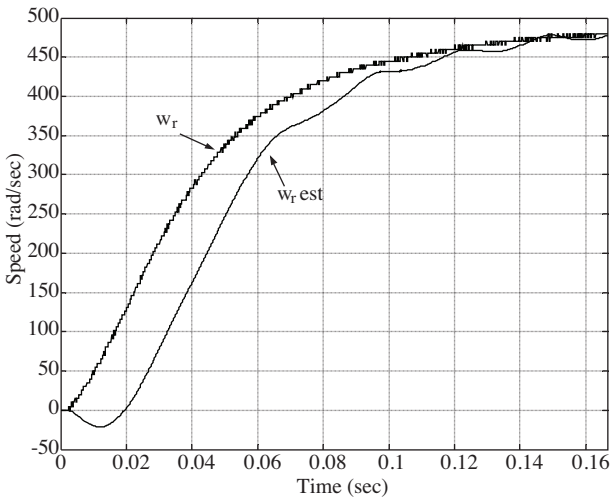

Figure 12. The estimated and the measured speed for 250 rpm reference speed.

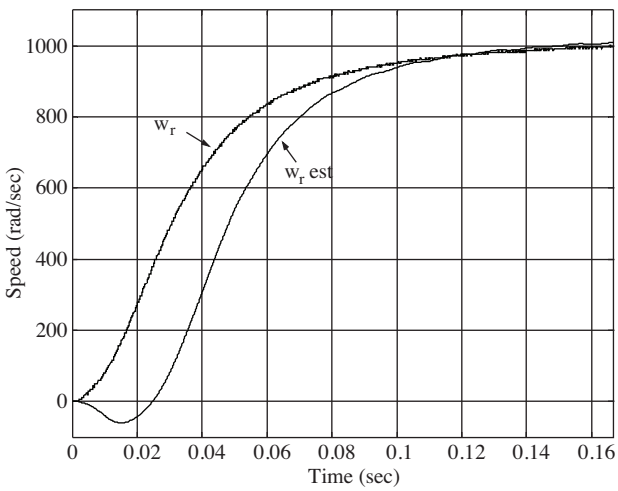

Figure 13. The estimated and the measured speed for 500 rpm reference speed.

4. Conclusion

Online parameter adaptation is an essential technique for improving static and dynamic performance of adjustable-speed drive systems with wide speed ranges, such as those in electric and hybrid vehicles. A novel Luenberger-sliding mode observer with online adaptation was developed to estimate the rotor time constant of an induction motor in an adjustable-speed drive system. The Luenberger component is predetermined by the machine model, while the sliding-mode component provides robustness in the case of large parameter variations.

The parameter estimation and adaptation algorithm were verified by simulation and experimental studies. The results show that the steady state performance of the observer is quite successful. Estimated speed nearly followed the measured speed. In the transient state, on the other hand, the observer was not able to track the real measured speed. This undesired effect can be compensated for with a soft start. A space vector modulation algorithm was preferred instead of the hysteresis current control algorithm, and it was implemented in DSP. Implementation of the proposed algorithm is simpler and less time-consuming, since a part of the observer is predetermined from the motor model.

Entries of the observer gain matrix are constituted with constant values. These entries can take different values for different speed regions. As part of further investigation, the authors propose using neural network, fuzzy-neural, or genetic algorithms in order to determine gain matrix coefficients as a better solution to the sensorless control problem.

References

[1] K. Hasse, "Zum Dynamischen Verhalten der Asynchronmachine bei Betrieb mit variable Standerfrequenz und Standerspannung," ETZ-A, Bd. 89, H. 4, pp. 77-81, 1968.

[2] F. Blaschke, "Das Prizip der Feldorientierung, Die Grundlage fur die TRNSVEKTOR-Regelung von Asynchnmachinen," Siemens Zeitschrift, Vol. 45, p. 757, 1971.

[3] R. Joetten, G. Maeder, "Control methods for good dynamic performance induction motor drives based on current and voltage as measured quantities", IEEE Trans. on Ind. Appl., Vol. 19, pp. 356-363, 1983.

[4] S. Sangwongwanic, S. Doki, T. Yonemoto, S. Okuma, "Adaptive sliding observer for direct field-oriented control of induction motors", Int. Conf. on Ind. Elec. Cont. and Instr., IECON'90, pp. 915-920, 1990.

[5] M.A. Brdys, T. Du, "Algorithms for joint state and parameter estimation in induction motor drive systems", International Conference on Control '91, Vol. 2, pp. 915-920, 1991.

[6] P. Vas, A.F. Stronach, M. Neuroth, "A fuzzy-controlled speed-sensorless induction motor drive with flux estimators", 7th International Conference on Electrical Machines and Drives, pp. 315-319, 1995.

[7] M. Abrate, G. Griva, F. Profumo, A. Tenconi, "High speed sensorless fuzzy-like Luenberger observer", 30th Annual IEEE Power Electronics Specialists Conference, PESC 99, Vol. 1, pp. 477-481, 1999.

[8] K.B. Lee, J.Y. Yoo, J.H. Song, I. Choy, "Improvement of low speed operation of electric machine with an inertia identification using ROELO", Electric Power Applications, IEE Proceedings, Vol. 151, pp. 116-120, 2004.

[9] M.A. Valenzuela, J.A. Tapia, J.A. Rooks, "Thermal evaluation of TEFC induction motors operating on frequency-controlled variable-speed drives", IEEE Trans. Ind. Appl., Vol. 40, pp. 692-698, 2004.

[10] T.H. Bishop, "Temperature monitoring is key to motor reliability", Maint. Technol. Mag., p. 34, 2004.

[11] A.K. Pradeep, J.P. Lyons, S.R. MacMinn, "Application of sliding mode observer for state estimation in rotating machines", Proc. VARSCON'91, pp. 57-64, 1991.

[12] P.L. Jansen, C.O. Thompson, R.D. Lorenz, "Observer-based direct field orientation for both zero and very high speed operation", Proc. of Power Conv. Conf., PCC Yokohama, pp. 432-437, 1993.

[13] F. Alogne, T. Raimondi, "Indirect adaptive speed control of induction motor systems based on model reference identifiers", Proc. IECON'93, Vol. 2, pp. 1035-1040, 1995.

[14] M.G. Aydeniz, I. Senol, "A novel approach to sensorless control of induction motors", ELECO 2009, 6th International Conference on Electrical and Electronics Engineering, Vol. 1, pp. 179-184, 2009.